Supporting Information for

Structural Insights into Inhibition of the Drug Target Dihydroorotate Dehydrogenase by Bacterial Hydroxyalkylquinolines

Samantha M. Horwitz,[a] Tamra C. Blue,[a] Joseph A. Ambarian,[a] Shotaro Hoshino,[b] Mohammad R. Seyedsayamdost,[b] and Katherine M. Davis*[a]

[a] Department of Chemistry, Emory University, Atlanta, GA 30322, USA
[b] Departments of Chemistry, Princeton University, Princeton, NJ 08544, USA

Table of Contents

References

Materials and Methods

Materials

Unless otherwise noted, all chemicals were obtained from Sigma-Aldrich. HMNQ was isolated from *B. thailandensis* as described below. Vector pET28a(+) encoding *E. coli* DHODH was obtained from Twist Bioscience.

Expression and Purification of EcDHODH

Expression and purification procedures were adapted from those described by *Björnberg et al*.[1] A kanamycin-resistant pET28a(+) vector containing the *Ec*DHODH gene with an N-terminal 6xHis tag was transformed into chemically-competent BL21(DE3) *E. coli* cells for expression. Cells were grown in 25 g/L LB broth containing 50 mg/mL kanamycin at 37°C and shaken at 240 rpm until they reached an OD_{600} ~0.6-0.8. The cultures were then cooled on ice for thirty minutes. After returning to room temperature, protein expression was induced by adding IPTG to a final concentration of 1 mM, and cultures were incubated at 18°C and 220 rpm for an additional 16 hours. Cells were subsequently harvested via centrifugation at 9000 g for 15 minutes, flash frozen in liquid nitrogen, and stored at -80°C.

All purification steps were performed at 4°C to ensure protein stability. In a representative purification, a 45 g cell pellet was thawed in 220 mL of lysis buffer (50 mM sodium phosphate, 0.25 mM EDTA, pH 8) and phenyl-methyl-sulfonyl-fluoride (PMSF) was added to a final concentration of 1 mM. Cells were lysed via sonication (15 seconds on, 15 seconds off for 30 minutes total at 50% amplitude and 4 °C), after which $MgCl_2$ and Triton-X were added to final concentrations of 5 mM and 0.2%, respectively. The lysed cells were left on ice for 30 minutes before centrifuging at 33000 g for 1 hour. The supernatant was subsequently loaded onto Co^{2+}-NTA resin, equilibrated with 10 column volumes (CVs) of buffer A (50 mM sodium phosphate, 0.1 mM EDTA, 0.1% Triton-X, 10 mM imidazole, pH 8). The column was first washed with 30 mM imidazole in buffer A before elution with 300 mM imidazole. The eluate was concentrated and buffer exchanged into buffer B (20 mM HEPES, 200 mM NaCl, pH 7.8) for further purification via size-exclusion. *Ec*DHODH was isocratically eluted from a Superdex 16x100 column preequilibrated in buffer B, and fractions were analyzed via SDS-PAGE. The purest fractions were subsequently combined, concentrated and exchanged into the storage buffer (25 mM sodium phosphate, 100 mM EDTA, pH 7.0 with 10% glycerol), yielding 19 mg of pure DHODH per L culture.

Purification of HMNQ

Burkholderia thailandensis E264 was streaked onto LB agar from a glycerol stock and incubated overnight at 30 °C. Then, a small piece of agar was transferred into 125 ml Erlenmeyer flask containing 25 ml LB broth and the flask was shaken at 30 °C and 200 rpm for 24 h. Large Fernbach flasks (3 x 2.8 L), each containing 1.0 L of LB broth supplemented with 50 mM MOPS (pH = 7.0) and 15 μM trimethoprim, were inoculated with the overnight culture (0.5% inoculum, v/v) and shaken at 30 °C and 200 rpm for 32 h.

The 3 L culture was centrifuged and the supernatant was loaded onto a solid-phase extraction Phenomenex Strata® C18-E column to adsorb hydrophobic compounds including HMNQ. Elution was carried out sequentially with 5 CV of 0%, 10%, 20%, 50% and 100% MeOH (in H_2O, v/v), and HMNQ eluted in the 100% MeOH fraction. This fraction was evaporated to dryness and loaded onto a silica gel column (10 mL, equilibrated with chloroform). Elution was carried out

sequentially with 3 CV of 0%, 1%, 2%, 5% and 10% MeOH (in chloroform, v/v), and HMNQ eluted in the chloroform (= 0% MeOH) fraction. This fraction was concentrated *in vacuo* and once more loaded onto a silica gel column (10 mL, equilibrated with chloroform), and eluted with 3 CV of 0%, 1%, 2%, 5% and 10% MeOH (in chloroform, v/v). Finally, 5.0 mg of HMNQ was obtained by evaporating 2% MeOH fraction to dryness. Identity and purity of HMNQ was verified by analysis via NMR and high-resolution mass spectrometry (HR-MS, Figure S1).

^{1}H NMR data of HMNQ (methanol-d_4, 500 MHz): δ 8.26 (1H, d, J = 8.0 Hz), 7.67 (1H, t, J = 8.0 Hz), 7.57 (1H, d, J = 8.0 Hz), 7.38 (1H, t, J = 8.0 Hz), 5.55-5.63 (2H, m), 3.52-3.57 (2H, m), 2.17 (3H, s), 2.07 (2H, m), 1.21-1.41 (8H, m), 0.88 (3H, t, J = 7.0 Hz). ^{13}C NMR data of HMNQ (methanol-d_4, 125 MHz): δ 178.2, 149.8, 139.2, 133.8, 131.3, 124.8, 123.7, 123.2, 123.1, 117.3, 115.3, 35.0, 32.1, 31.4, 28.9, 28.4, 22.3, 13.0, 9.3.

Crystallization of holo EcDHODH, inhibitor and ubiquinone surrogate complexes

All crystals of *Ec*DHODH were grown using the hanging drop vapor diffusion method at room temperature. To obtain crystals of the N-terminally His$_6$-tagged holo *Ec*DHODH, a solution containing 20 mg/mL His$_6$-tagged *Ec*DHODH in storage buffer was mixed 1:1 with a precipitant solution of 1.6 M sodium malonate, pH 7.1-7.3, and 19-23% (w/v) PEG3350 to generate a final drop volume of 4 μL. Yellow plate-like crystals appeared within 24 hours and were fully formed within 3 days (~100 x 100 μm^2). The crystals were looped and transferred briefly into cryoprotectant, comprised of the precipitant plus 25% (v/v) glycerol, before flash freezing in liquid nitrogen.

Crystals of the HMNQ- and HQNO-bound complexes were produced via a similar procedure. However, to improve reproducibility, a seed stock was generated following the appearance of holo *Ec*DHODH crystals by transferring one crystal-containing drop into 13.5 μL of a 1:1 protein/precipitant solution (generated by combining 54 μL of *Ec*DHODH at 13 mg/mL and 54 μL of reservoir solution). This mixture was vortexed in 30 second intervals for a total of 3 minutes, and dilutions of this seed stock were produced using the same 1:1 protein/precipitant solution. Square yellow plate-like crystals appeared within 48 hours and appeared fully formed within 1 week (~75 x 75 μm^2). Drops at the 10^{-4} dilution were subsequently incubated with a small volume (<0.25 μL) of HMNQ (100 mM) and DHO (100 mM) overnight, while those at the 10^{-5} dilution were spiked with a small volume of 100 mM HQNO (purchased from Fisher Scientific) and DHO (100 mM). The respective crystals were then looped into cryoprotectant containing 30% (v/v) ethylene glycol and flash frozen in liquid nitrogen.

To obtain the DCIP-bound structure, crystals of N-terminally His$_6$-tagged *Ec*DHODH were grown by combining a 20 mg/mL solution of the enzyme in storage buffer 1:1 with a reservoir solution containing 2.4 M DL-malic acid, pH 7.2, to a final drop volume of 4 μL. Star-like yellow crystal clusters formed within 24 hours, and the crystals grew to conjoined plates within a week (~75 x 75 μm^2). Drops were spiked with >0.25 uL of 100 mM DCIP (purchased from Fisher Scientific) for 1 hour before being looped, transferred into cryoprotectant containing 30% ethylene glycol, and flash frozen in liquid nitrogen.

X-ray Data Collection and Processing

Diffraction data were collected at beamline 23-ID-B of the Advance Photon Source at Argonne National Laboratory using an Eiger X 16M (Dectris) detector. Crystals were maintained at 100 K to minimize X-ray-induced damage while images were collected sequentially (Δφ = 0.2°) with an incident wavelength of 1.033 Å. The data were subsequently indexed, integrated and scaled using

XDS before merging with AIMLESS.[2, 3] The structure of *Ec*DHODH in complex with the natural product inhibitor HQNO was solved via molecular replacement with PHASER using the structure of holo *Ec*DHODH (PDB accession code: 1F76) as the search model.[4,5] All other structures were solved via isomorphous replacement. I.e. the HQNO-bound model, which had the highest resolution, was refined against each of the other data sets. The same R_{free} flags were maintained across all data sets, and PDB_REDO was used to ensure unbiased refinement.[6] Model building was then conducted in Coot,[7] and structures were refined in Phenix.[8] Coordinates and restraints for HMNQ were generated with JLigand.[9] Model quality was assessed using Molprobity.[10]

Although DHO was soaked into the crystals from which the inhibitor-bound structures were solved, the reaction product ORO was ultimately modelled into the final structures. This decision was made based on the results from the liquid-liquid extraction assay portrayed in Figure S4 depicting the appearance of a peak in the *Ec*DHODH sample not present in the DHO standard. Furthermore, the presence of ORO in the crystal structures can be rationalized mechanistically. Despite the fact that DHO has a higher affinity than ORO for the oxidized enzyme—that is, the enzyme before the reduction of FMN by the substrate—it has been shown in anaerobic stopped-flow experiments that ORO dissociates too slowly from the reduced enzyme to be catalytically relevant,[11] suggesting that an oxidizing cosubstrate is necessary to drive product dissociation. The absence of oxidizing cosubstrate in all of the structures solved supports the assignment of ORO as the species present in the active site.

All structures were in the $C222_1$ space group and contain two molecules in the asymmetric unit. The final model of holo *Ec*DHODH (PDB accession code: 7T6H) was refined to 2.42 Å resolution. The final models of the HQNO-bound enzyme (PDB accession code: 7T5K), the HMNQ-bound enzyme (PDB accession code:7T5Y), and the DCIP-bound enzyme (PDB accession code:7T6C) were refined to 2.25 Å, 2.62 Å, and 2.53 Å resolution, respectively. Selected data processing and refinement statistics can be found in Table S1. Figures depicting the structures were generated with PyMol, while 2-D interaction diagrams were produced using LIGPLOT.[12]

Docking Methods

Docking models were generated using the SwissDock server, which predicts possible interactions between a target protein and associated small molecules without bias toward a defined site.[13] Given minimal differences between the solved structures, the respective ligands were docked into the highest resolution *Ec*DHODH model (PDB accession code: 7T5K) following removal of all small molecules and solvent. A model for a truncated ubiquinone construct terminated at the fifth carbon of the alkyl chain was obtained by extracting the associated coordinates from PDB accession code 7RJB. Docking models with the highest FullFitness rank were used for the analysis of ligand binding in comparison to the X-ray crystal structures.

GC-MS Methods

The presence of orotate bound to as-purified *Ec*DHODH was determined by gas chromatography-mass spectrometry (GC-MS) analysis (GCMS-QP2010SE, Shimadzu Scientific Instruments, Kyoto, Japan). Purified *Ec*DHODH, prepared as described above, was buffer exchanged to remove glycerol and concentrated to 134 mg/mL. A small volume of concentrated protein was then added in a 2:1 ratio with 1% DMSO in ethyl acetate. The tube was shaken and centrifuged for 3 minutes, after which the organic layer was carefully pipetted into a GC vial for loading onto the GC-MS. The DHO standard was generated by dissolving 150 mM of substrate in

DMSO. This stock was subsequently diluted in ethyl acetate such that the final concentration of DMSO was 1%.

Assay mixtures were separated on an Agilent J&W Cyclodex-B capillary column (30 m × 320 μm × 0.25 μm) at a column inlet pressure of 100 kPa and column flow rate of 1.00 mL/min with a split ratio of 1:100. The injection, ion, and interface temperatures were set to 200°C, while the oven temperature was initially set to 110°C for 10 min and was increased linearly to 200°C over the course of 20 minutes. Solutions were run with an injection volume of 1 μL. After GC-MS analysis it was apparent that the mass peaks for DHO were not present in the holo *Ec*DHODH (Figure S4). Unfortunately, due to ORO's well-known high polarity and poor ionization,[14] we were unable to directly test for its presence by GC-MS or by HPLC-MS.

In order to confirm that ORO is unable to dissociate and exchange with DHO in the absence of ubiquinone or a suitable surrogate, we conducted an additional GC/MS assay: DHODH (103 mg/mL) was incubated overnight with excess DHO (200 mM) followed by buffer exchange to remove unbound substrate. Like with the as-purified material, we did not observe a peak corresponding to DHO substantiating this hypothesis (Figure S4).

Table S1. Crystallographic data processing and refinement statistics for *Ec*DHODH structures.

PDB ID (ligand)	7TCH	7T5K (HQNO)	7T5Y (HMNQ)	7T6C (DCIP)
Data Collection[a]				
Space group	C222$_1$	C222$_1$	C222$_1$	C222$_1$
Unit cell (Å)	a = 104.53, b = 169.50, c = 129.98	a = 104.05, b = 169.33, c = 129.97	a = 104.05, b = 169.33, c = 129.97	a = 104.05, b = 169.33, c = 129.97
	α = β = γ = 90	α = β = γ = 90	α = β = γ = 90	α = β = γ = 90
Wavelength (Å)	1.0332	1.0332	1.0332	1.0332
Resolution range (Å)	48.49 – 2.42 (2.51 – 2.42)	48.30 – 2.25 (2.33 -2.25)	48.30 – 2.63 (2.72 – 2.63)	48.30 – 2.53 (2.62 – 2.53)
Total observations	332357	405663	255674	287405
Total unique observations	43993	54501	34399	38184
I/σ$_1$	8.06 (1.30)	9.34 (1.09)	9.91 (0.88)	9.19 (1.42)
Completeness (%)	99.2 (99.2)	99.6 (98.8)	99.1 (93.4)	98.76 (89.23)
R$_{merge}$	0.158 (1.63)	0.116 (1.39)	0.173 (1.89)	0.170 (1.32)
R$_{pim}$	0.0613 (0.6226)	0.0456 (0.541)	0.0673 (0.742)	0.0652 (0.510)
Redundancy	7.6 (7.7)	7.4 (7.4)	7.4 (7.2)	7.5 (7.4)
Refinement Statistics				
Resolution range (Å)	48.49 – 2.42	48.30 – 2.25	48.30 – 2.63	48.30 – 2.25
Reflections (total)	43983	54473	34354	38172
Reflections (test)	1615	2001	1259	1399
Total atoms refined	5351	5323	5268	5340
Solvent	134	133	82	110
R$_{work}$ (R$_{free}$)	0.1987 (0.2350)	0.2164 (0.2325)	0.2107 (0.2406)	0.2008 (0.3197)
RMSDs				
Bond lengths (Å)/angles (°)	0.009/1.15	0.011/1.31	0.010/1.02	0.005/0.79
Ramachandran plot				
Favored/allowed (%)	96.54/3.31	97.75/2.10	96.70/3.15	97.00/2.85
Mean B values (Å^2)				
Protein chains A/B	55.29/58.97	58.08/61.87	61.31/64.77	54.05/56.65
ORO/FMN/ligands	64.74/50.39/--	75.82/52.28/65.42	64.51/54.45/67.27	66.27/50.92/68.60
Solvent	54.77	57.08	63.59	54.58

[a] Values in parentheses refer to the high-resolution shell.
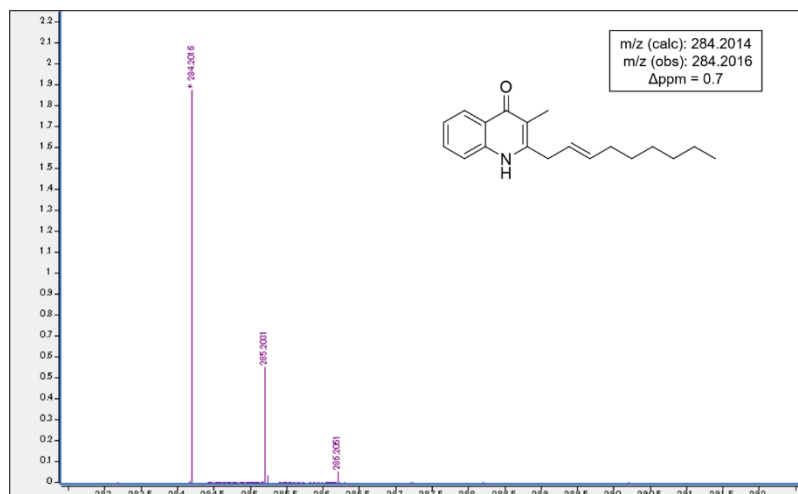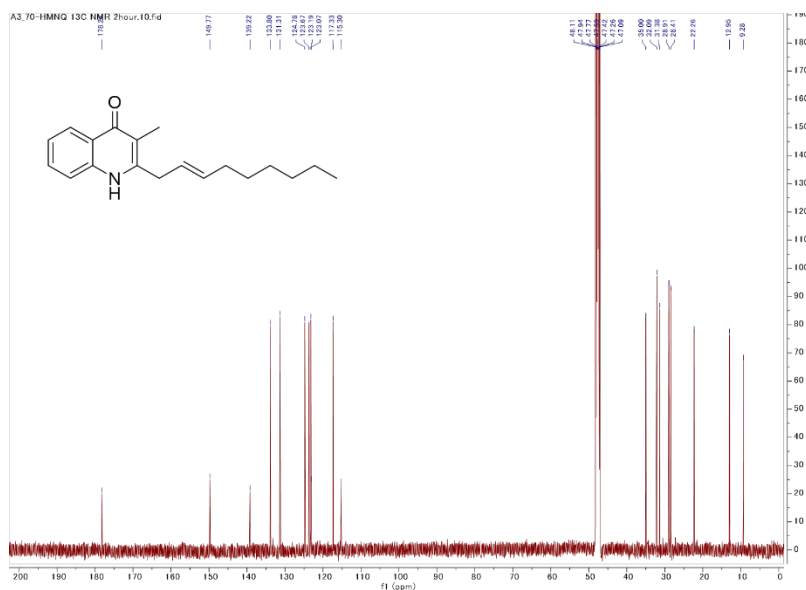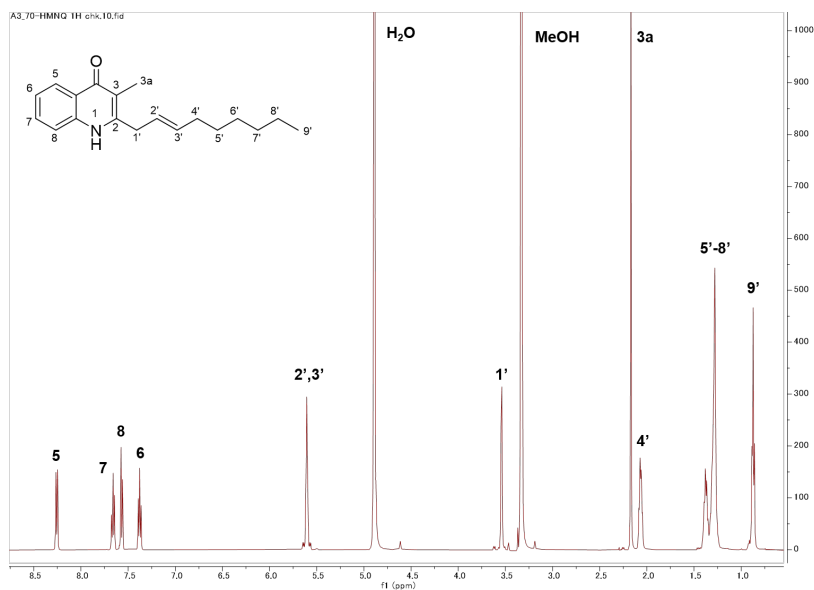
Figure S1. ^{1}H NMR (top) and ^{13}C NMR (middle) spectra of isolated HMNQ in methanol-d_4 at 500 MHz and 125 MHz, respectively. The spectra confirm the identify of HMNQ. HR-MS analysis of isolated HMNQ (bottom). The calculated and observed HR-MS data are shown and are entirely consistent with the HMNQ structure.

m/z (calc): 284.2014
m/z (obs): 284.2016
Δppm = 0.7
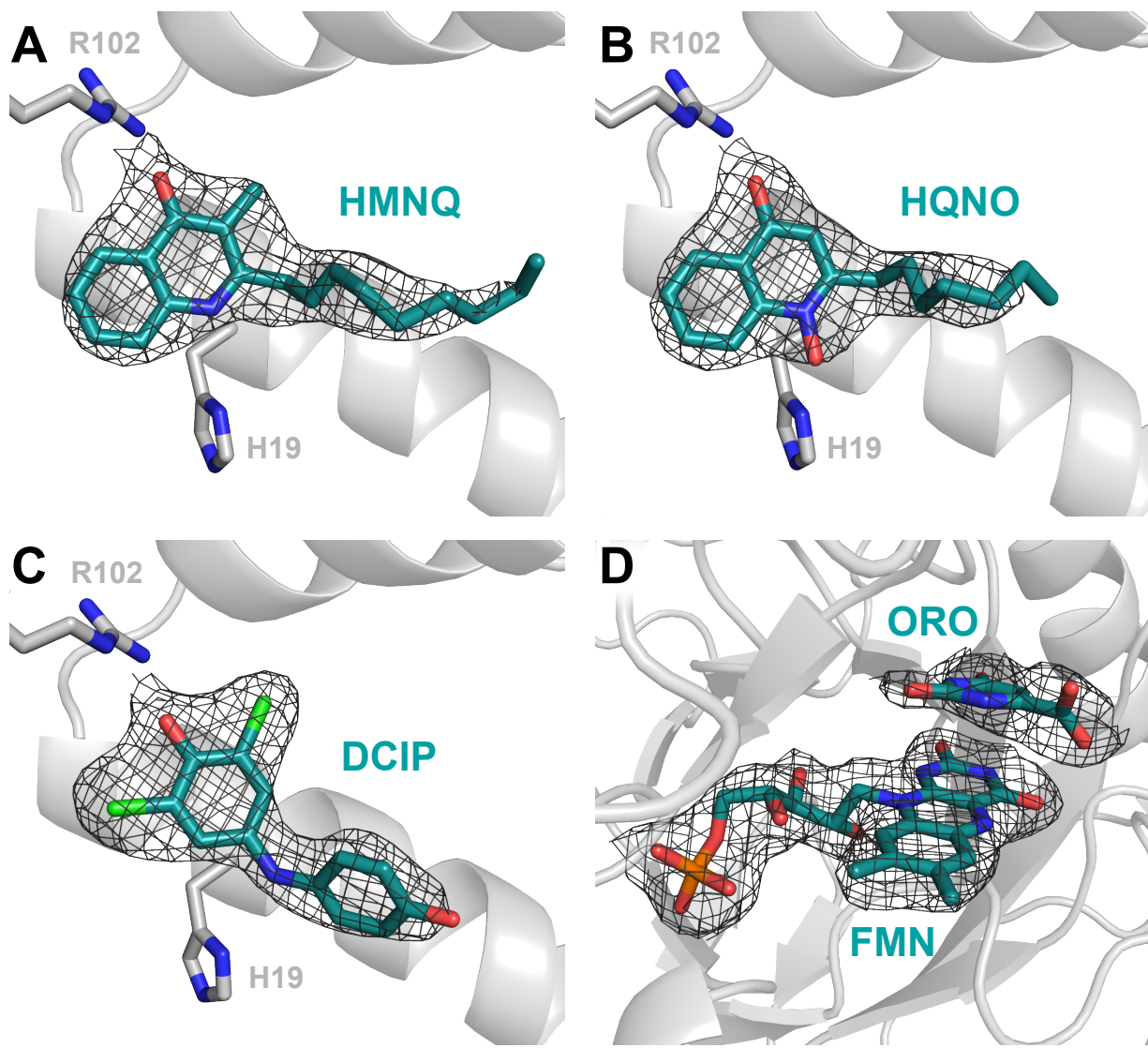
Figure S2. $2F_o - F_c$ electron density maps associated with the ligands contoured at 1.0σ.

Figure S3. Binding mode of FMN (A) and the π-stacking interaction (B) with ORO (C).
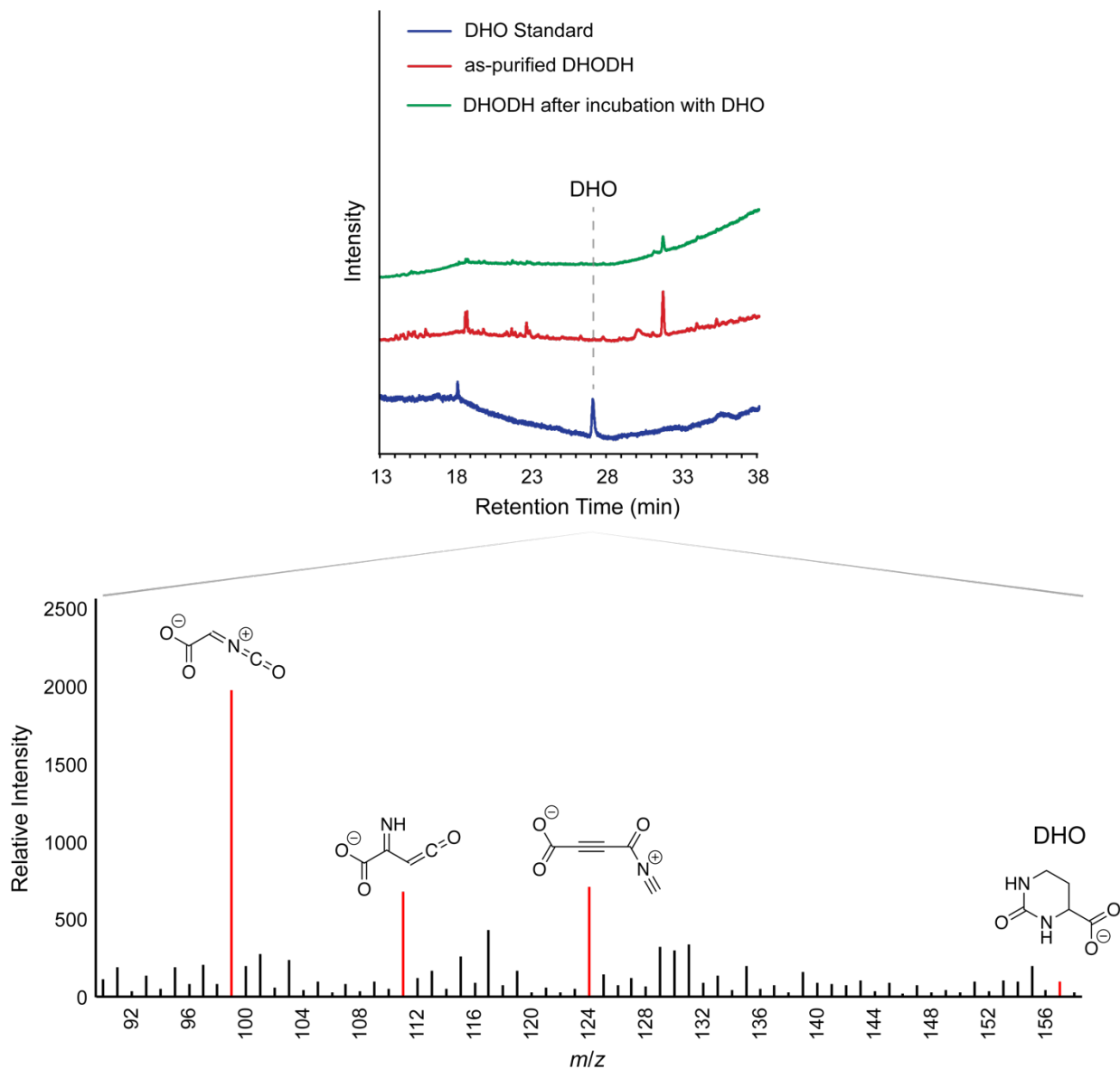
Figure S4. GC-MS analysis interrogating the presence of DHO in DHODH samples used for crystallization. Shown are total ion chromatograms as a function of retention time for a DHO standard (blue trace), as-purified DHODH (red trace), and DHODH incubated with DHO (green trace). The DHO peak, identified by the mass-to-charge ratio, is marked and a mass spectrum is presented. Relevant, expected fragments that are characteristic of DHO are shown in red.
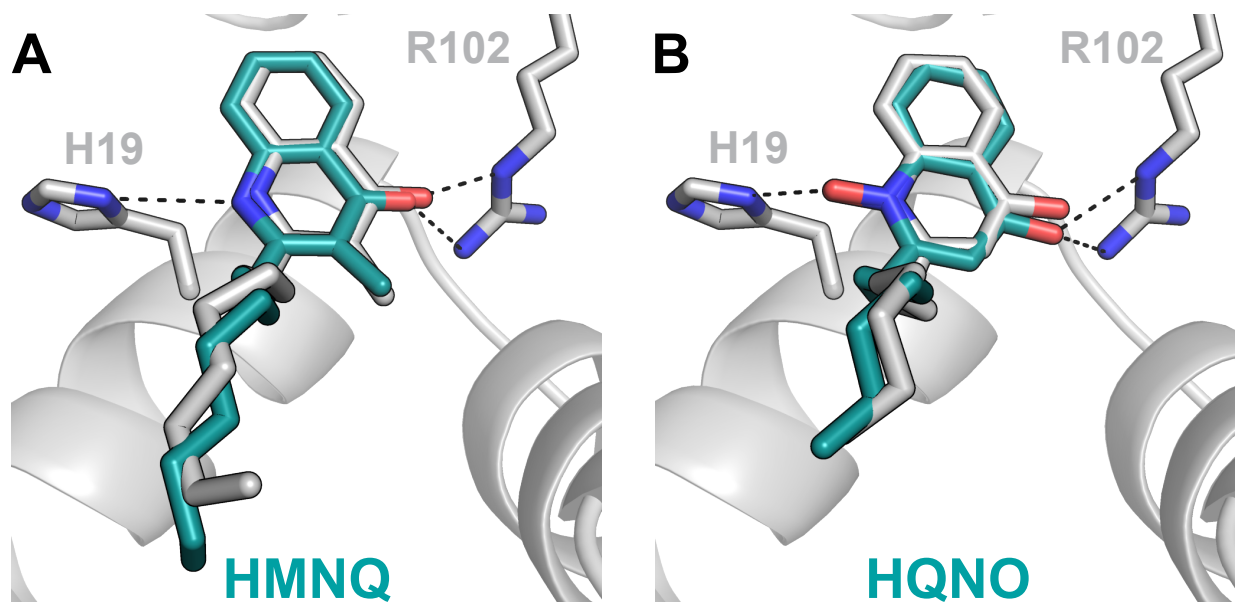
Figure S5. Overlay of crystallographic (grey) and docking models for HMNQ (A) and HQNO (B).

References

1.   O. Björnberg, A. C. Grüner, P. Roepstorff and K. F. Jensen, *Biochemistry*, 1999, **38**, 2899-2908.
2.   W. Kabsch, *Acta Crystallogr. D*, 2010, **66**, 125-132.
3.   P. R. Evans and G. N. Murshudov, *Acta Crystallogr. D*, 2013, **69**, 1204-1214.
4.   A. J. McCoy, R. W. Grosse-Kunstleve, P. D. Adams, M. D. Winn, L. C. Storoni and R. J. Read, *J. Appl. Crystallogr.*, 2007, **40**, 658-674.
5.   S. Nørager, K. F. Jensen, O. Björnberg and S. Larsen, *Structure*, 2002, **10**, 1211-1223.
6.   R. P. Joosten, K. Joosten, G. N. Murshudov and A. Perrakis, *Acta crystallogr. D*, 2012, **68**, 484-496.
7.   P. Emsley, B. Lohkamp, W. G. Scott and K. Cowtan, *Acta Crystallogr. D*, 2010, **66**, 486-501.
8.   P. D. Adams, P. V. Afonine, G. Bunkóczi, V. B. Chen, I. W. Davis, N. Echols, J. J. Headd, L. W. Hung, G. J. Kapral, R. W. Grosse-Kunstleve, A. J. McCoy, N. W. Moriarty, R. Oeffner, R. J. Read, D. C. Richardson, J. S. Richardson, T. C. Terwilliger and P. H. Zwart, *Acta Crystallogr. D*, 2010, **66**, 213-221.
9.   A. A. Lebedev, P. Young, M. N. Isupov, O. V. Moroz, A. A. Vagin and G. N. Murshudov, *Acta Crystallogr. D*, 2012, **68**, 431-440.
10. C. J. Williams, J. J. Headd, N. G. Moriarty, M. G. Prisant, L. L. Videau, L. N. Deis, V. V. Verma, D. A. Keedy, B. J. Hintze, V. B. Chen, S. Jain, S. M. Lewis, B. W. Arendall, J. Snoeyink, P. D. Adams, S. C. Lovell, J. S. Richardson and D. C. Richardson, *Protein Sci.*, 2018, **27**, 293-315.
11. B. A. Palfey, O. Björnberg and K. F. Jensen, *Biochemistry*, 2001, **40**, 4381-4390.
12. A. C. Wallace, R. A. Laskowski and J. M. Thornton, *Protein Eng. Des. Sel.*, 1995, **8**, 127-134.
13. A. Grosdidier, V. Zoete and O. Michielin, *Nucleic Acids Res.*, 2011, **39**, W270-W277.
14. R. Hušková, P. Barták, L. Čáp, x, D. Friedecký and T. Adam, *J. Chromatogr. B*, 2004, **799**, 303-309.